

Reduced Order Isogeometric Analysis Approach for PDEs in Parametrized Domains

Fabrizio Garotta^{*1}, Nicola Demo^{†2}, Marco Tezzele^{‡2},
Massimo Carraturo^{§1}, Alessandro Reali^{¶1}, and Gianluigi Rozza^{||2}

¹Department of Civil Engineering and Architecture Università degli Studi di Pavia, Pavia, Italy

²Mathematics Area, mathLab, SISSA, International School of Advanced Studies, via Bonomea 265, I-34136 Trieste, Italy

June 5, 2022

Abstract

In this contribution, we coupled the isogeometric analysis to a reduced order modelling technique in order to provide a computationally efficient solution in parametric domains. In details, we adopt the free-form deformation method to obtain the parametric formulation of the domain and proper orthogonal decomposition with interpolation for the computational reduction of the model. This technique provides a real-time solution for any parameter by combining several solutions, in this case computed using isogeometric analysis on different geometrical configurations of the domain, properly mapped into a reference configuration. We underline that this reduced order model requires only the full-order solutions, making this approach non-intrusive. We present in this work the results of the application of this methodology to a heat conduction problem inside a deformable collector pipe.

1 Introduction

Nowadays, in the industrial and engineering fields, as well as in the biomedical sciences, fast and accurate simulations are crucial in several applications,

^{*}fabrizio.garotta01@universitadipavia.it

[†]nicola.demo@sissa.it

[‡]marco.tezzele@sissa.it

[§]massimo.carraturo01@universitadipavia.it

[¶]alereali@unipv.it

^{||}gianluigi.rozza@sissa.it

such as, for example, shape design optimization and real-time patient specific diagnosis and control. To this end many reduced order modelling (ROM) techniques have been developed in the last decade [41, 8, 32, 38, 37]. We cite among others reduced basis methods [22, 35], proper orthogonal decomposition (POD) [10], proper generalized decomposition [9], and hierarchical model reduction [28, 29, 4]. Reduced order modelling can be integrated to various high fidelity methods such as finite element [33], spectral element, or finite volume methods [21, 46, 47]. We do mention also recent features of the reduced methods able to provide useful algorithms for uncertainty quantification as well as data science and better exploitation of high performance computing [50, 7].

Reduced order methods allow a fast and reliable approximation of parameterized PDEs by constructing small-sized approximation spaces. Using these spaces for the discretization of the original problem, it is possible to build a reduced order model that is a sufficiently accurate approximation of the original full order problem. The fundamental characteristic that makes the method functional from an engineering and industrial point of view is that the offline phase (more expensive), where the actual analysis is carried out, is performed only once in high performance computing (HPC) structures and then remains. The online phase exploits the calculations already performed and therefore a small computational power, like the one of laptops or portable devices, is sufficient. This ensures real-time processing of the problem without having to access HPC facilities for the analysis of new parameters.

ROM is crucial in industrial simulation-based design optimization problems in naval and nautical engineering [50, 16], but also in biomedical applications for coronary bypass [3, 2] and carotid occlusions [48] for example.

The focus of this work is to embed in a ROM framework the isogeometric analysis (IGA) [23, 12, 11] for the simulation of heat diffusion inside a collector pipe. The proposed approach is integrated in a numerical pipeline with efficient geometrical parameterization of the domain through free form deformation (FFD) [42, 24], an IGA solver as high fidelity discretization, and POD with interpolation (PODI) [6, 40, 34] for a fast evaluation of the solution field at untested parameters. Figure 1 depicts the schema of the complete computational pipeline.

We chose FFD instead of other general purpose geometrical parameterization techniques such as radial basis functions (RBF) interpolation [5, 27, 25], or inverse distance weighting (IDW) interpolation [43, 54, 20, 1], because of the possibility to use only few parameters to deform the entire domain of interest.

The IGA approach allows to integrate classical finite element analysis (FEA) into conventional industrial CAD tools. To this end IGA directly employs standard CAD representation bases, e.g., B-splines or Non-uniform

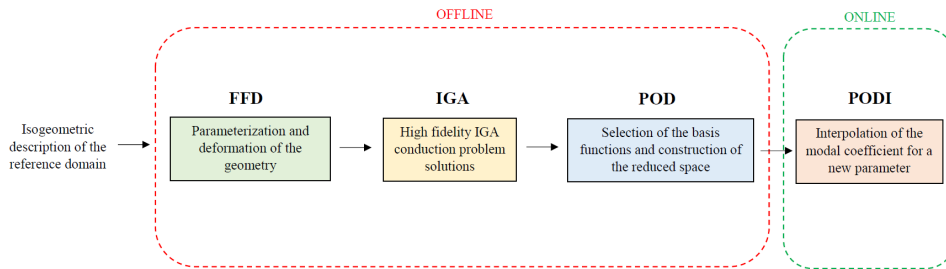


Figure 1: Offline-online numerical pipeline. We consider the heat conduction problem described by PDEs defined on parametrized geometry. The parametrization of the geometry is managed through the FFD which allows the realization of different deformation settings. In the offline stage we first solve a full order model using IGA to derive the solutions and then, we create a ROM applying the POD as space reduction technique. Finally, through the PODI, in the online stage we look for the real-time solution of the reduced problem for a new parameter.

rational B-splines (NURBS), as basis for the analysis. In this way we can avoid the classical mesh generation and the consequent geometrical approximation error, obtaining a direct design-to-analysis simulation, since we are employing the same class of functions for both the geometry parameterization and the solution fields approximation. In this context, the IGA is ideal for solving elliptic and parabolic PDEs on domains of very general shape. However, when the objective is to solve the same problem repeatedly on different domains, the cost of setting up the problem (meshing, matrix assembly) every time from scratch can be too high. An optimal solution to this problem is a reduction of the model.

Previous IGA-ROMs works were developed in the last years [26, 39, 55], but we underline that the novelty of this work is related to the POD with interpolation integration into the numerical pipeline, for a non-intrusive approach. Even if in this work we present a proof of concept we stress the fact that it can play an important role for the integration with industrial CAD files being independent from the IGA full order solver used.

2 The parametrized heat conduction problem inside a collector pipe

The problem of interest we are going to solve throughout this work is a parametrized heat diffusion problem inside a collector pipe.

Let $\Omega \subset \mathbb{R}^2$ be a domain that describes an idealized collector pipe in 2D, as shown in Figure 2. We will refer to Ω as the reference domain, and for

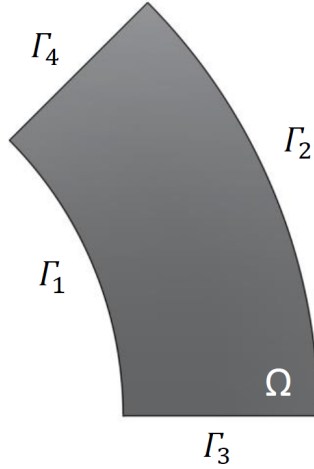


Figure 2: Idealized collector pipe representation scheme in 2D. Ω represents with internal domain of interest, while $\Gamma_{1,\dots,4}$ indicate the different boundaries. In particular Γ_3 is the inlet, and Γ_4 is the outlet.

practical reasons it represents the undeformed geometry.

We also introduce $\mathbb{D} \subset \mathbb{R}^m$ which is our parameter space, and for convenience it will be an hypercube. For every $\mu \in \mathbb{D}$, which is a vector of geometrical parameters describing a particular deformation of the domain, we can define a shape morphing map $\mathcal{M}(x; \mu) : \mathbb{R}^2 \rightarrow \mathbb{R}^2$. We will indicate the deformed domain as $\Omega(\mu) = \mathcal{M}(\Omega; \mu)$. We refer to Section 4 for the specific characterization of such mapping.

The parametrized heat diffusion problem reads: find $u(\mu)$ such that

$$\begin{cases} \Delta u(\mu) = 0 & \text{in } \Omega(\mu) \\ u(\mu) = 0 & \text{in } \Gamma_{1,2,4} \\ \nabla u(\mu) \cdot n = g & \text{in } \Gamma_3, \end{cases} \quad (1)$$

where u is the temperature distribution inside the domain, and g represents the prescribed heat flux at the inlet. The Dirichlet boundary conditions describe a perfect insulator with no flux. For sake of simplicity from now on $g = 1$.

We can introduce the weak formulation of the problem (1). We denote with

$$V = H_{0_{124}}^1(\Omega) := \{v \in H^1(\Omega) \text{ such that } v|_{\Gamma_1, \Gamma_2, \Gamma_4} = 0\}$$

the Sobolev space for the temperature. Multiplying the first equation of the system by a test function and integrating by parts we obtain the following problem: given $\mu \in \mathbb{D}$, find $u \in V$ such that

$$a(u, v; \mu) = L(v; \mu) \quad \forall v \in V, \quad (2)$$

where the bilinear form $a(u, v; \mu)$, and the linear form $L(v; \mu)$, are defined as follows

$$a(u, v; \mu) = \int_{\Omega} \nabla u(\mu) \nabla v \, dV \quad \forall u, v \in V, \quad (3)$$

$$L(v; \mu) = \int_{\Gamma_3} g v \, dS \quad \forall v \in V. \quad (4)$$

3 Isogeometric paradigm for both the geometry and the solution field

Usually a CAD representation of the domain is obtained through B-splines or NURBS, which are able to exactly describe all conic sections. Here we are going to briefly present both.

It is possible to derive the B-spline basis functions of order p using Cox-de Boor's recursion formula [13, 14]

$$N_{i,p}(\xi) = \frac{\xi - \xi_i}{\xi_{i+p} - \xi_i} N_{i,p-1}(\xi) + \frac{\xi_{i+p+1} - \xi}{\xi_{i+p+1} - \xi_{i+1}} N_{i+1,p-1}(\xi), \quad (5)$$

where

$$N_{i,0}(\xi) = \begin{cases} 1 & \text{if } \xi_i \leq \xi < \xi_{i+1}, \\ 0 & \text{otherwise,} \end{cases} \quad (6)$$

and $\Xi = \{\xi_1, \xi_2, \dots, \xi_{n+p+1}\}$ is the knot vector, a non-decreasing set of coordinates with $\xi_i \in \mathbb{R}$, and n is the number of basis functions which comprise the B-spline. B-spline curves in \mathbb{R}^d are constructed by taking a linear combination of B-spline basis functions. The vector valued coefficients of the basis functions are referred to as *IGA control points*. Given n basis functions $\{N_{i,p}\}_{i=1}^n$ of order p , and the corresponding control points P_i , a piecewise polynomial B-spline curve is given by

$$C(\xi) = \sum_{i=1}^n P_i N_{i,p}(\xi). \quad (7)$$

IGA control points are points that define the so called control mesh, which is a mesh made up by the multilinear elements that define and control the geometry of the problem. It is important to emphasize that the control mesh does not coincide with the actual geometry of the physical domain. The control points can be considered as the analog of the nodal coordinates of the finite element method, with the difference that, in IGA contest they represent the coefficients of the basis functions of a B-spline having non-interpolatory nature. A generalization of B-splines are the NURBS, which are a rational version of them and can thus represent exactly any kind of

geometry. This feature of NURBS allows to bypass altogether the computationally expensive mesh generation and refinement cycle and at the same time to preserve the exact geometry of the CAD model. The key insight of IGA is to use the geometrical map of the NURBS representation as a basis for the push forward used in the analysis. NURBS basis functions of order p are defined through B-spline basis functions as

$$R_{i,p}(\xi) = \frac{N_{i,p}(\xi)w_i}{W(\xi)} = \frac{N_{i,p}(\xi)w_i}{\sum_{j=1}^n N_{j,p}(\xi)w_j}, \quad (8)$$

where w_i are the associated weights. Taking a linear combination of basis functions and control points, we express a NURBS curve as

$$C(\xi) = \sum_{i=1}^n P_i R_{i,p}(\xi). \quad (9)$$

The isoparametric concept is utilized for both FEA and IGA. However, the difference between FEA and IGA lies in the bases employed for the analysis. In IGA, the inputs for the calculations come from a CAD model defined by NURBS curves, which can be used directly for analysis, while in FEA the finite element mesh is generated starting from an approximation of the original geometry. The mapping from the parametric domain to the physical domain is then given by

$$x = \sum_{k=1}^n R_k(\xi)P_k, \quad (10)$$

where $R_k(\xi)$ are the NURBS basis functions, n is the number of control points, ξ the parametric coordinate and P_k is the k -th control point. In an isoparametric formulations the displacement field is approximated by the same shape functions formally:

$$u = \sum_{k=1}^n R_k(\xi)u_k, \quad (11)$$

where u_k is the value of the displacement field at the control point P_k . It is therefore referred to as a control variable or more generally a degree of freedom.

In Figure 3 we present the IGA representation of the domain Ω we described in section 2. In red the six IGA control points defining the NURBS curves. In particular the knot vectors Ξ and H are defined as follows:

$$\begin{aligned} \Xi &= \{0, 0, 1, 1\} & k &= 2 \quad p = 1, \\ H &= \{0, 0, 0, 1, 1, 1\} & k &= 3 \quad p = 2, \end{aligned}$$

where k and p respectively indicate the multiplicity and the degree of the polynomial ($k = p + 1$).

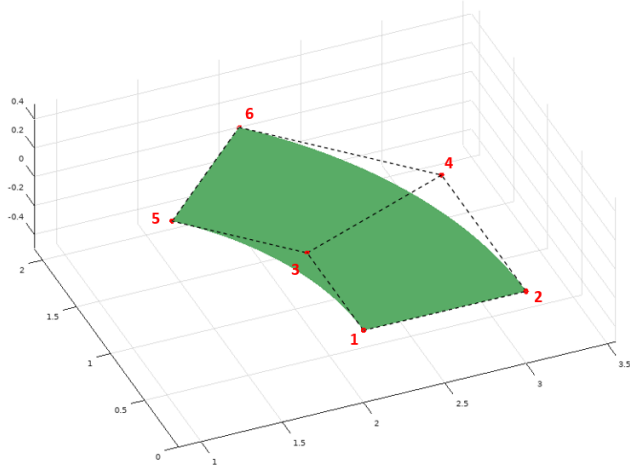


Figure 3: Idealized 2D collector pipe and its IGA control points mesh. The six control points are indicated with red dots.

4 Shape parameterization and deformation through free form deformation

The FFD method has been proposed in [42]. It was initially used as a tool for computer-assisted geometric design and animation, nowadays instead it is mostly adopted in academia, industry and several engineering application fields as morphing technique for complex geometries thanks to its features [17, 49, 51, 44]. In the FFD procedure, the object to be deformed is embedded into a rectangular lattice of points, then some of these points are moved to deform the whole embedded domain. This technique has three main benefits: *(i)* with few parameters — the displacement of the lattice points — it is possible to perform global deformations, *(ii)* it allows to preserve continuity also in the surface derivatives and *(iii)* it is completely independent with respect to the object, so it results applicable also to computational grids [24].

Initially, FFD maps the original domain Ω to the reference one using the affine map ψ defined as $\psi : D \rightarrow [0, 1]^n$, where $D \supset \Omega$ is the parallelepiped containing the domain and n is the number of dimensions. We select a regular grid of control points P in the unitary hypercube and we perturb the space by moving these points. The displacements, the so called FFD weights, control the basis functions whose tensor product constitute the deformation map \hat{T} . We underline that it is also possible to move only some points: typically we fix several rows/columns of control points to obtain desired levels of continuity and to fix certain parts of the domain.

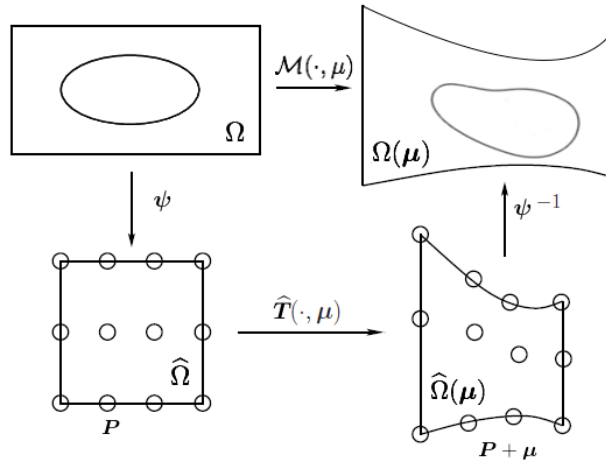


Figure 4: Schematic diagram of the free form deformation map $\mathcal{M}(\cdot, \mu)$, of the control points $P_{i,k}$, and the resulting deformation when applied to the original domain Ω . $\mathcal{M}(\cdot, \mu)$ is the composition of the three maps presented: ψ , \hat{T} , and ψ^{-1} .

Finally, we need the back mapping to the physical domain, that is the map ψ^{-1} . Formally, we obtain the FFD map as the composition of the three maps, i.e. $\mathcal{M}(\cdot, \mu) := (\psi \circ \hat{T} \circ \psi^{-1})(\cdot, \mu)$, where μ refers to the parametric displacement of the control points (see Figure 4 for a schematic summary).

It must be remarked that, although FFD is characterized by high flexibility and easiness of handling, it suffers from some limitations. The first lies in the fact that the design variables may have no physical significance: they are defined in a parametric domain that can not be expressed into a particular unit of measurement by definition. Moreover all the control points are restricted to lie on a regular lattice and, in that way, local refinements could not be performed.

In this work, we apply the FFD to parametrize the initial 2D domain. We embed the domain with a square lattice of length 3, using 2×2 control points. The lattice origin coincides with the axes origin. We use two different parameters that are the displacement along the x direction of the FFD control points P_{11} and P_{12} depicted in Figure 5. In particular we define $\mathbb{D} := [-0.3, 0.3]^2$. We use Bernstein polynomials as basis function to deform the geometry in the reference domain. In Figure 5 we present on the left the undeformed configuration of the idealized collector pipe, where in red we highlight the IGA control points, while the white big dots are the FFD control points. On the right there is just an example of deformation corresponding to a displacement of 0.4 for P_{11} and -0.5 for P_{12} , for now on express as $\mu = (0.4, -0.5)$.

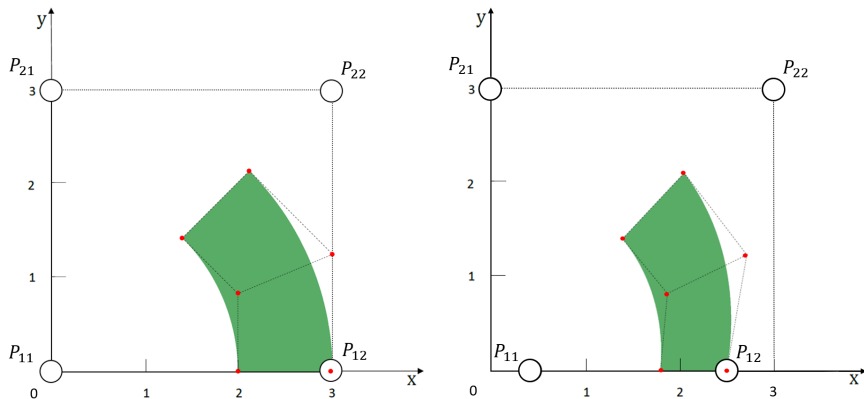


Figure 5: The initial unperturbed domain (left) and an example of deformed domain (right) using the FFD technique with $\mu = (0.4, -0.5)$. The red dots are the NURBS control points, the white big dots are the FFD control points.

5 Data-driven reduced order modelling by proper orthogonal decomposition with interpolation

The reduced basis (RB) method is a computational reduction technique allowing to quickly and accurately obtain the solution of parametric PDEs. The need to solve parameterized differential problems, possibly in a very rapid calculation time, emerges in various contexts, particularly when we are interested in characterizing the response of a system in numerous scenarios or operating conditions [36, 35, 30, 32]. The goal of an RB approximation is the representation of the full-order problem as combination of the (few) essential characteristics of the problem itself. In this way the dimensions are considerably lower than those of a problem discretized with a classic Galerkin method. Any discretization leading to a large system to be solved to achieve a certain accuracy is referred to as *high fidelity* (or *full order*) *approximation*. The basic idea of an RB approximation is a computationally efficient solution of the parametric problem keeping the approximation error lower than a given tolerance. In particular, the aim is to approximate the solution of a parametric PDE using a very small number of degrees of freedom instead of the large number required by an high fidelity approximation.

To do this, the full order problem is solved only for a few instances of the input parameters during the computationally expensive *offline* phase. The so stored snapshots are used in the *online* phase for the approximation of the solution for any new parameter. The generation of the snapshots database can be done only once and it is completely decoupled from any new input-output calculation related to a new parameter. The online phase exploits the calculations already performed and therefore not necessary of a

large computational power. This ensures real-time processing of the problem without having to use high performance computing infrastructures for analysis, which can be instead run on a simple laptop with limited computational power.

In this work, we adopt a complete data-driven model order reduction called proper orthogonal decomposition with interpolation (PODI). PODI is applicable using only the system output — so also experimental data — without requiring the equations of the original problem. Especially in the industrial context, this is a big benefit: it allows to preserve the *know how* and to be completely independent from the full-order solver. We list some examples of PODI applications [40, 6, 8, 22].

PODI aims to approximate the solution manifold by interpolating the snapshots collected in the offline phase. Since for high-dimensional data the interpolation can be very expensive, we use proper orthogonal decomposition (POD) to project the original snapshots onto a low-rank space. POD allows to define a subspace approximating the original data in an optimal least squares sense by using the singular value decomposition (SVD) algorithm [53, 31, 45]. We consider a set of n_{train} snapshots $s_1, \dots, s_{n_{\text{train}}} = s(\mu_1), \dots, s(\mu_{n_{\text{train}}}) \in V^{\mathcal{N}}$, where $V^{\mathcal{N}}$ is the high-dimensional space and \mathcal{N} refers to its dimension. We define the snapshots matrix \mathbf{S} as the matrix that contains the snapshots in the columns $\mathbf{S} = [s_1 \ \dots \ s_{n_{\text{train}}}]$. We apply the SVD to \mathbf{S} :

$$\mathbf{S} = \mathbf{V}\mathbf{\Sigma}\mathbf{W}^*, \quad (12)$$

where

$$\mathbf{V} = [\zeta_1 \ \dots \ \zeta_{n_{\text{train}}}] \in \mathbb{C}^{\mathcal{N} \times n_{\text{train}}}, \quad (13)$$

$$\mathbf{W} = [\Psi_1 \ \dots \ \Psi_{n_{\text{train}}}] \in \mathbb{C}^{n_{\text{train}} \times n_{\text{train}}}, \quad (14)$$

are orthogonal matrices whose columns are the left and right singular vectors of \mathbf{S} respectively, and

$$\mathbf{\Sigma} = \text{diag}(\sigma_1 \ \dots \ \sigma_{n_{\text{train}}}) \in \mathbb{C}^{n_{\text{train}} \times n_{\text{train}}}, \quad (15)$$

is a diagonal matrix such that $\sigma_1 \geq \sigma_2 \geq \dots \geq \sigma_{n_{\text{train}}} \geq 0$ are the computed singular values of \mathbf{S} . The POD modes of dimension N are defined as the first N left singular vectors of \mathbf{S} , that correspond to the N largest singular values

$$\mathbf{Z} = [\zeta_1 \ \dots \ \zeta_N]. \quad (16)$$

Now we project the original snapshots onto the space spanned by the modes: the snapshots are so described as linear combination of the modes such that

$$s_i = \sum_{j=1}^N \mathbf{C}_{j,i} \zeta_j \quad \text{for } i = 1, \dots, n_{\text{train}}, \quad (17)$$

where the columns of matrix \mathbf{C} are called *modal coefficients*. We can compute these coefficients as $\mathbf{C} = \mathbf{Z}^T \mathbf{S}$, where $\mathbf{C} = [c_1 \dots c_{n_{\text{train}}}] \in \mathbb{R}^{N \times n_{\text{train}}}$. We remark the relation between these coefficients and the parameters; hence we can interpolate the modal coefficients to compute the coefficient for any new point belonging to the parameter space. Finally, using the modes, we are able to approximate the new high-dimensional solution.

Since the PODI technique relies on interpolation, the accuracy of the approximated solution depends mostly by the chosen interpolation method.

6 Numerical Results

In order to construct the reduced order model, we firstly need to sample the solution manifold using several high-fidelity snapshots. We select 100 different configurations applying the FFD technique to the initial domain. The parameters μ are equispaced in the parameter space $[-0.3, 0.3] \times [-0.3, 0.3]$. This strategy allows us to cover the entire parametric space with a linear interpolation.

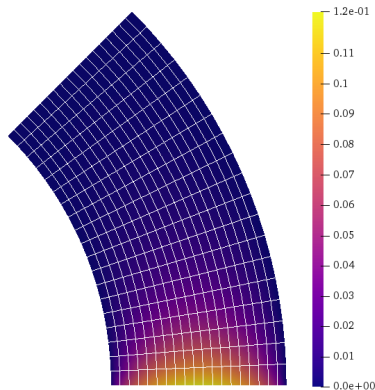


Figure 6: The adopted computational grid and the graphical representation of the numerical solution of the Laplace problem for the undeformed configuration.

For each configuration, IGA is performed testing *GeoPDEs* [15, 52], an open source and free package introduced in 2010 by Rafael Vázquez, written in Octave and fully compatible with Matlab. In GeoPDEs the IGA is efficiently implemented in its classic Galerkin version. For the resolution of the full-order problem we created a mesh with 400 degrees of freedom. Figure 6 shows the graphical representation of the numerical solution.

Once the snapshots are collected, we create the reduced order model using the PODI method. The modes are so computed by applying the SVD algorithm to the snapshots matrix. We show in Figure 7 the obtained

singular values: we note that the first one retains $\sim 96\%$ of the total energy, while the 10th singular value is below 10^{-6} . We expect that even with only few modes we can generate a reduced order model introducing only a negligible error.

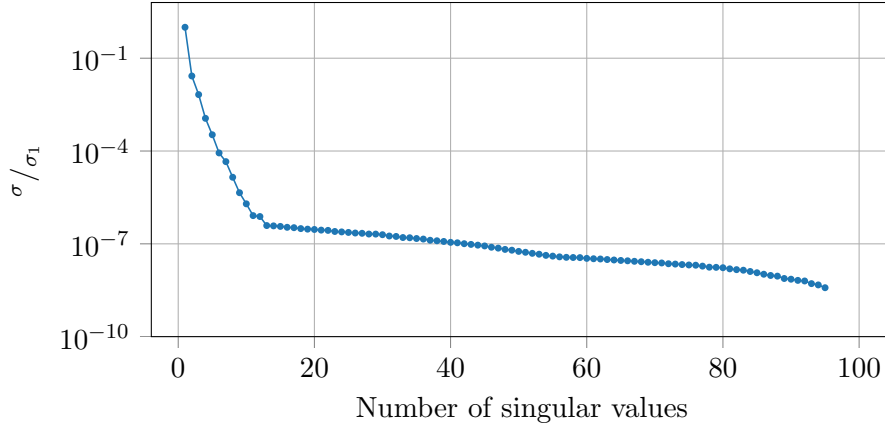


Figure 7: The singular values obtained by the snapshots matrix using the SVD technique.

Using the modes, we can calculate the modal coefficients by projecting the original snapshots. Hence, we can approximate any new solution in the parametric space through the interpolation of the modal coefficients. Among the various interpolation techniques we choose *linear interpolation*. We report an example where the reduced solution is calculated for the undeformed object by setting the parameter to zero. In Figure 8 a visual comparison between the high-fidelity solution and the reduced one is presented: it is very intuitive to note that the two solutions are almost identical.

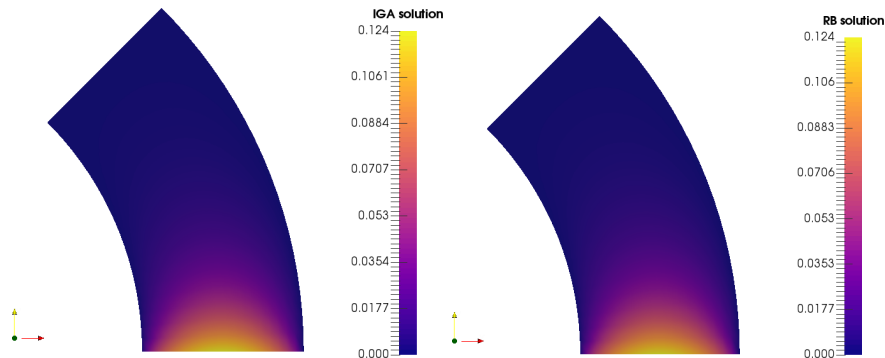


Figure 8: Comparison between the full-order solution (left) and the reduced order model solution (right) for the undeformed configuration.

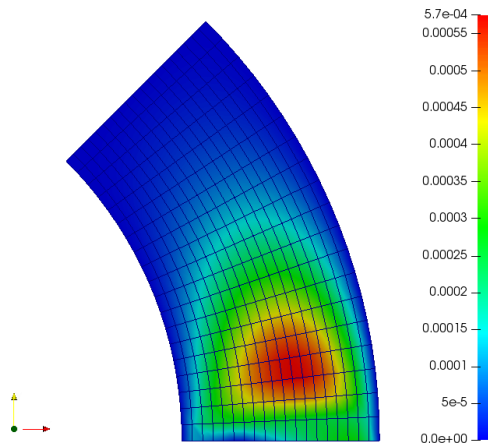


Figure 9: Error between the full-order solution and the reduced order solution for the unperturbed configuration. The different color corresponds to ascending values of the error. The error gradually increases from the blue zone to the red zone where there is the greatest diffusive heat effect. The results show how, even in the red zone, the error assumes acceptable values.

In Figure 9 instead we can see the error between the reduced solution and the IGA solution. We calculate the error $e(\mu)$ as follows

$$e(\mu) = |u_{\mathcal{N}}(\mu) - u_N(\mu)|. \quad (18)$$

The maximum error is around 6×10^{-4} so it is possible to state that it is an acceptable error.

We can also evaluate the a posteriori error committed on a test dataset. A posteriori error estimation allows to minimize the dimension N of the snapshot database used to generate the reduced space and to quantify the error of the approximation with respect to the number of modes selected. The error is calculated computing the relative L^2 norm of the difference between the approximated solution obtained using PODI approach and the IGA truth solution, on a test dataset composed by high fidelity solutions corresponding to 20 uniformly distributed random samples in the parameter space. The plots in Figure 10 show the relative error against the dimension of the database and the number of modes. We see that 100 samples and only 4 modes are enough for an average error below 10^{-3} . We refer to [19] for a posteriori error bounds in an RB-IGA setting.

Finally, we can evaluate the performance improvement obtained using ROM by calculating the speedup S_p as

$$S_p = \frac{u_{\mathcal{N}}(s)}{u_N(s)}, \quad (19)$$

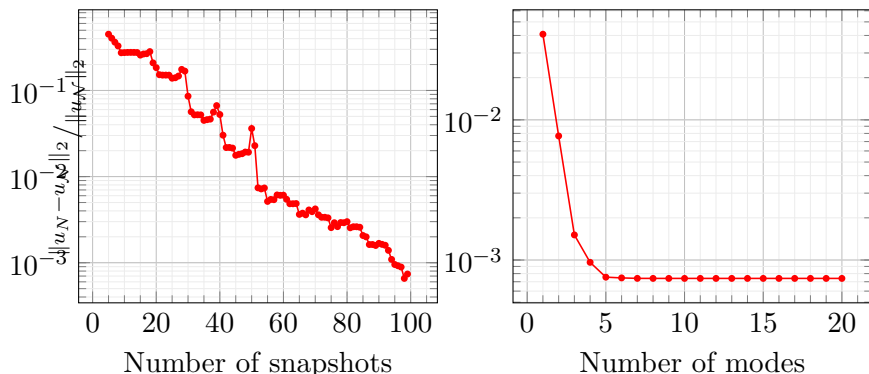


Figure 10: A posteriori L^2 relative error between the reduced order solution and the high fidelity one, computed on the test dataset composed by 20 uniformly distributed random samples in the parameter space. On the left the error with respect to the dimension of the offline database. On the right the error trend varying the number of modes selected. With only 4 modes we obtain an average relative error below 10^{-3} .

where we divide the time in seconds needed to compute the full order solution by the time needed for the reduced one. Due to the different size of the systems, the difference of computational time is remarkable even if, for this test-case, the full-order problem is very simple. We measured the computational time required by the two techniques on the same machine, and for different parameter values, and we obtained a mean speedup of approximately 1000. Concerning the software involved, for the model order reduction we adopted EZyRB [18], which is a Python library for ROM, based on barycentric triangulation for the selection of the parameter points and on POD for the selection of the modes. The software uses a non-intrusive approach in which the solutions are projected on the low dimensional space then interpolated for the approximation of the solution.

7 Conclusions and future developments

In this work we presented a complete non-intrusive computational pipeline involving geometrical parameterization through free form deformation, iso-geometric analysis, and reduced order model, for fast and reliable field evaluation. We applied this pipeline to a diffusion problem in an idealized 2D collector pipe. We used a data-driven non-intrusive approach for the model order reduction, that is the proper orthogonal decomposition with interpolation. This setting, even if tested on a simple problem, will allow us to deal with more complex industrial CAD files, since we used a geometrical parameterization technique independent from the object of interest, and the ROM chosen uses only the snapshots of the IGA high fidelity simulations.

Results and speedup achieved look promising to continue with the implementation of more complex problems on 3D geometries. The effectiveness of an RB approach would be exploited even better increasing the complexity of the simulation in cases where a large number of analysis has to be computed, e.g. in parameter optimization studies. The developed RB-IGA method is thus interesting from both academic and industrial points of view. As a matter of fact, since IGA is directly interfaced with CAD, an undergoing development of the work is the implementation of a dedicated software based on the RB-IGA method, allowing real-time evaluations of outputs of interest for different NURBS parameterizations.

Acknowledgments

This work was partially funded by the project SOPHYA, “Seakeeping Of Planing Hull YAchts”, supported by Regione FVG, POR-FESR 2014-2020, Piano Operativo Regionale Fondo Europeo per lo Sviluppo Regionale, and partially supported by European Union Funding for Research and Innovation — Horizon 2020 Program — in the framework of European Research Council Executive Agency: H2020 ERC CoG 2015 AROMA-CFD project 681447 “Advanced Reduced Order Methods with Applications in Computational Fluid Dynamics” P.I. Gianluigi Rozza.

This work was also partially supported by Fondazione Cariplo - Regione Lombardia through the project “Verso nuovi strumenti di simulazione super veloci ed accurati basati sull’analisi isogeometrica”, within the program RST - rafforzamento.

References

- [1] F. Ballarin, A. D’Amario, S. Perotto, and G. Rozza. A POD-Selective Inverse Distance Weighting method for fast parametrized shape morphing. *Int. J. Num. Meth. Eng.*, in press, 2018.
- [2] F. Ballarin, E. Faggiano, S. Ippolito, A. Manzoni, A. Quarteroni, G. Rozza, and R. Scrofani. Fast simulations of patient-specific haemodynamics of coronary artery bypass grafts based on a POD–Galerkin method and a vascular shape parametrization. *Journal of Computational Physics*, 315:609–628, 2016.
- [3] F. Ballarin, E. Faggiano, A. Manzoni, A. Quarteroni, G. Rozza, S. Ippolito, C. Antona, and R. Scrofani. Numerical modeling of hemodynamics scenarios of patient-specific coronary artery bypass grafts. *Biomechanics and Modeling in Mechanobiology*, 16(4):1373–1399, 2017.

- [4] D. Baroli, C. M. Cova, S. Perotto, L. Sala, and A. Veneziani. Hi-POD solution of parametrized fluid dynamics problems: preliminary results. In *Model Reduction of Parametrized Systems*, pages 235–254. Springer, 2017.
- [5] M. D. Buhmann. *Radial basis functions: theory and implementations*, volume 12. Cambridge university press, 2003.
- [6] T. Bui-Thanh, M. Damodaran, and K. Willcox. Proper Orthogonal Decomposition extensions for parametric applications in compressible aerodynamics. In *21st AIAA Applied Aerodynamics Conference*, page 4213, 2003.
- [7] P. Chen, A. Quarteroni, and G. Rozza. Reduced basis methods for uncertainty quantification. *SIAM/ASA Journal on Uncertainty Quantification*, 5:813–869, 2017.
- [8] F. Chinesta, A. Huerta, G. Rozza, and K. Willcox. *Model Order Reduction: a survey*. Wiley Encyclopedia of Computational Mechanics, 2016.
- [9] F. Chinesta, R. Keunings, and A. Leygue. *The proper generalized decomposition for advanced numerical simulations: a primer*. Springer Science & Business Media, 2013.
- [10] E. A. Christensen, M. Brøns, and J. N. Sørensen. Evaluation of proper orthogonal decomposition-based decomposition techniques applied to parameter-dependent nonturbulent flows. *SIAM Journal on Scientific Computing*, 21(4):1419–1434, 1999.
- [11] J. A. Cottrell, T. J. Hughes, and Y. Bazilevs. *Isogeometric Analysis: toward integration of CAD and FEA*. John Wiley & Sons, 2009.
- [12] J. A. Cottrell, T. J. Hughes, and A. Reali. Studies of refinement and continuity in isogeometric structural analysis. *Computer methods in applied mechanics and engineering*, 196(41-44):4160–4183, 2007.
- [13] G. Cox Maurice. The numerical evaluation of B-splines. *IMA Journal of Applied Mathematics*, 10(2):134–149, 1972.
- [14] C. De Boor. On calculating with B-splines. *Journal of Approximation theory*, 6(1):50–62, 1972.
- [15] C. De Falco, A. Reali, and R. Vázquez. GeoPDEs: a research tool for Isogeometric Analysis of PDEs. *Advances in Engineering Software*, 42(12):1020–1034, 2011.

- [16] N. Demo, M. Tezzele, G. Gustin, G. Lavini, and G. Rozza. Shape optimization by means of proper orthogonal decomposition and dynamic mode decomposition. In *Technology and Science for the Ships of the Future: Proceedings of NAV 2018: 19th International Conference on Ship & Maritime Research*, pages 212–219. IOS Press, 2018.
- [17] N. Demo, M. Tezzele, A. Mola, and G. Rozza. An efficient shape parametrisation by free-form deformation enhanced by active subspace for hull hydrodynamic ship design problems in open source environment. In *The 28th International Ocean and Polar Engineering Conference, ISOPE*, 2018.
- [18] N. Demo, M. Tezzele, and G. Rozza. EZyRB: Easy Reduced Basis method. *The Journal of Open Source Software*, 3(24):661, 2018.
- [19] D. Devaud and G. Rozza. volume 119, chapter Certified Reduced Basis Method for Affinely Parametric Isogeometric Analysis NURBS Approximation. Springer, 2017.
- [20] D. Forti and G. Rozza. Efficient geometrical parametrisation techniques of interfaces for reduced-order modelling: application to fluid–structure interaction coupling problems. *International Journal of Computational Fluid Dynamics*, 28(3-4):158–169, 2014.
- [21] B. Haasdonk and M. Ohlberger. Reduced basis method for finite volume approximations of parametrized linear evolution equations. *ESAIM: Mathematical Modelling and Numerical Analysis*, 42(2):277–302, 2008.
- [22] J. S. Hesthaven, G. Rozza, and B. Stamm. *Certified Reduced Basis Methods for Parametrized Partial Differential Equations*. Springer Briefs in Mathematics. Springer, Switzerland, 1 edition, 2015.
- [23] T. J. Hughes, J. A. Cottrell, and Y. Bazilevs. Isogeometric Analysis: CAD, finite elements, NURBS, exact geometry and mesh refinement. *Computer methods in applied mechanics and engineering*, 194(39-41):4135–4195, 2005.
- [24] T. Lassila and G. Rozza. Parametric free-form shape design with PDE models and reduced basis method. *Computer Methods in Applied Mechanics and Engineering*, 199(23-24):1583–1592, 2010.
- [25] A. Manzoni, A. Quarteroni, and G. Rozza. Model reduction techniques for fast blood flow simulation in parametrized geometries. *International journal for numerical methods in biomedical engineering*, 28(6-7):604–625, 2012.

- [26] A. Manzoni, F. Salmoiraghi, and L. Heltai. Reduced Basis Isogeometric Methods (RB-IGA) for the real-time simulation of potential flows about parametrized NACA airfoils. *Computer Methods in Applied Mechanics and Engineering*, 284:1147–1180, 2015.
- [27] A. Morris, C. Allen, and T. Rendall. CFD-based optimization of aerofoils using radial basis functions for domain element parameterization and mesh deformation. *International Journal for Numerical Methods in Fluids*, 58(8):827–860, 2008.
- [28] S. Perotto, A. Ern, and A. Veneziani. Hierarchical local model reduction for elliptic problems: a domain decomposition approach. *Multiscale Modeling & Simulation*, 8(4):1102–1127, 2010.
- [29] S. Perotto, A. Reali, P. Rusconi, and A. Veneziani. Higamod: A hierarchical isogeometric approach for model reduction in curved pipes. *Computers & Fluids*, 142:21–29, 2017.
- [30] J. S. Peterson. The Reduced Basis Method for incompressible viscous flow calculations. *SIAM Journal on Scientific and Statistical Computing*, 10(4):777–786, 1989.
- [31] A. Quarteroni. *Numerical models for differential problems*, volume 2. Springer, 2009.
- [32] A. Quarteroni and G. Rozza. *Reduced Order Methods for Modeling and Computational Reduction*, volume 9 of *MS&A – Modeling, Simulation and Applications*. Springer, 2014.
- [33] A. Quarteroni, G. Rozza, and A. Manzoni. Certified reduced basis approximation for parametrized Partial Differential Equations and applications. *Journal of Mathematics in Industry*, 1(1):3, 2011.
- [34] M. Ripepi, M. Verveld, N. Karcher, T. Franz, M. Abu-Zurayk, S. Görtz, and T. Kier. Reduced-order models for aerodynamic applications, loads and MDO. *CEAS Aeronautical Journal*, 9(1):171–193, 2018.
- [35] G. Rozza, D. B. P. Huynh, and A. T. Patera. Reduced Basis Approximation and a posteriori error estimation for affinely parametrized elliptic coercive Partial Differential Equations. *Archives of Computational Methods in Engineering*, 15(3):1, 2007.
- [36] G. Rozza, T. Lassila, and A. Manzoni. Reduced basis approximation for shape optimization in thermal flows with a parametrized polynomial geometric map. In *Spectral and high order methods for Partial Differential Equations*, pages 307–315. Springer, 2011.

- [37] G. Rozza, M. H. Malik, N. Demo, M. Tezzele, M. Girfoglio, G. Stabile, and A. Mola. Advances in Reduced Order Methods for Parametric Industrial Problems in Computational Fluid Dynamics. Glasgow, UK, 2018. ECCOMAS.
- [38] F. Salmoiraghi, F. Ballarin, G. Corsi, A. Mola, M. Tezzele, and G. Rozza. Advances in geometrical parametrization and reduced order models and methods for computational fluid dynamics problems in applied sciences and engineering: overview and perspectives. Crete, Greece, 2016. ECCOMAS.
- [39] F. Salmoiraghi, F. Ballarin, L. Heltai, and G. Rozza. Isogeometric analysis-based reduced order modelling for incompressible linear viscous flows in parametrized shapes. *Advanced Modeling and Simulation in Engineering Sciences*, 3(1):21, 2016.
- [40] F. Salmoiraghi, A. Scardigli, H. Telib, and G. Rozza. Free-form deformation, mesh morphing and reduced-order methods: enablers for efficient aerodynamic shape optimisation. *International Journal of Computational Fluid Dynamics*, 0(0):1–15, 2018.
- [41] W. H. Schilders, H. A. Van der Vorst, and J. Rommes. *Model order reduction: theory, research aspects and applications*, volume 13. Springer, 2008.
- [42] T. Sederberg and S. Parry. Free-Form Deformation of solid geometric models. In *Proceedings of SIGGRAPH - Special Interest Group on GRAPHics and Interactive Techniques*, pages 151–159. SIGGRAPH, 1986.
- [43] D. Shepard. A two-dimensional interpolation function for irregularly-spaced data. In *Proceedings-1968 ACM National Conference*, pages 517–524. ACM, 1968.
- [44] D. Sieger, S. Menzel, and M. Botsch. On shape deformation techniques for simulation-based design optimization. In S. Perotto and L. Formaggia, editors, *New Challenges in Grid Generation and Adaptivity for Scientific Computing*, pages 281–303. Springer, 2015.
- [45] L. Sirovich. Turbulence and the dynamics of coherent structures. i. coherent structures. *Quarterly of applied mathematics*, 45(3):561–571, 1987.
- [46] G. Stabile, S. Hijazi, A. Mola, S. Lorenzi, and G. Rozza. POD-Galerkin reduced order methods for CFD using Finite Volume Discretisation: vortex shedding around a circular cylinder. *Communications in Applied and Industrial Mathematics*, 8(1):210–236, 2017.

- [47] G. Stabile and G. Rozza. Finite volume POD-Galerkin stabilised reduced order methods for the parametrised incompressible Navier–Stokes equations. *Computers & Fluids*, 173:273–284, sep 2018.
- [48] M. Tezzele, F. Ballarin, and G. Rozza. Combined parameter and model reduction of cardiovascular problems by means of active subspaces and POD-Galerkin methods. In *Mathematical and Numerical Modeling of the Cardiovascular System and Applications*. SEMA SIMAI Springer Series 16, 2018.
- [49] M. Tezzele, N. Demo, M. Gadalla, A. Mola, and G. Rozza. Model order reduction by means of active subspaces and dynamic mode decomposition for parametric hull shape design hydrodynamics. In *Technology and Science for the Ships of the Future: Proceedings of NAV 2018: 19th International Conference on Ship & Maritime Research*, pages 569–576. IOS Press, 2018.
- [50] M. Tezzele, N. Demo, A. Mola, and G. Rozza. An integrated data-driven computational pipeline with model order reduction for industrial and applied mathematics. *Submitted, Special Issue ECMI*, 2018.
- [51] M. Tezzele, F. Salmoiraghi, A. Mola, and G. Rozza. Dimension reduction in heterogeneous parametric spaces with application to naval engineering shape design problems. *Advanced Modeling and Simulation in Engineering Sciences*, 5(1):25, Sep 2018.
- [52] R. Vázquez. A new design for the implementation of isogeometric analysis in octave and matlab: Geopdes 3.0. *Comput. Math. Appl.*, 2016.
- [53] S. Volkwein. Proper Orthogonal Decomposition: Theory and reduced-order modelling. *Lecture Notes, University of Konstanz*, 4(4), 2013.
- [54] J. Witteveen and H. Bijl. Explicit mesh deformation using Inverse Distance Weighting interpolation. In *19th AIAA Computational Fluid Dynamics*. AIAA, 2009.
- [55] S. Zhu, L. Dedè, and A. Quarteroni. Isogeometric analysis and proper orthogonal decomposition for parabolic problems. *Numerische Mathematik*, 135(2):333–370, 2017.